LBL-18045

Lawrence Berkeley Laboratory

UNIVERSITY OF CALIFORNIA

RECEIVED
BERKELEY LABORATORY
AUG 20 1984
LIBRARY AND
DOCUMENTS SECTION

Materials & Molecular Research Division

Presented at the Ion Beam Modification of Materials Conference, Cornell University, Ithaca, NY, July 16-20, 1984; and to be published in Nuclear Instruments and Methods in Physics Research

ON THE ORIGINS OF STRUCTURAL DEFECTS IN BF_2^+-IMPLANTED AND RAPID-THERMALLY-ANNEALED SILICON: CONDITIONS FOR DEFECT-FREE REGROWTH

T. Sands, J. Washburn, E. Myers, and D.K. Sadana

July 1984

TWO-WEEK LOAN COPY
This is a Library Circulating Copy which may be borrowed for two weeks.

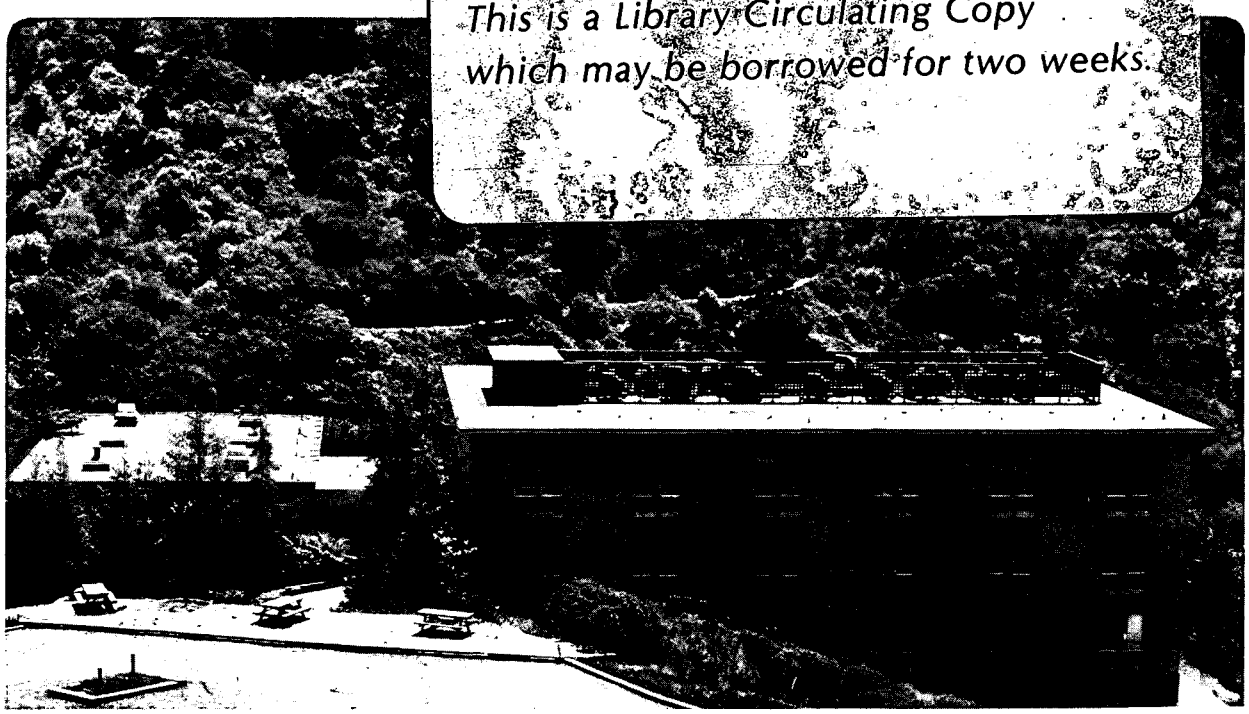

Prepared for the U.S. Department of Energy under Contract DE-AC03-76SF00098

LBL-18045

DISCLAIMER

This document was prepared as an account of work sponsored by the United States Government. While this document is believed to contain correct information, neither the United States Government nor any agency thereof, nor the Regents of the University of California, nor any of their employees, makes any warranty, express or implied, or assumes any legal responsibility for the accuracy, completeness, or usefulness of any information, apparatus, product, or process disclosed, or represents that its use would not infringe privately owned rights. Reference herein to any specific commercial product, process, or service by its trade name, trademark, manufacturer, or otherwise, does not necessarily constitute or imply its endorsement, recommendation, or favoring by the United States Government or any agency thereof, or the Regents of the University of California. The views and opinions of authors expressed herein do not necessarily state or reflect those of the United States Government or any agency thereof or the Regents of the University of California.

LBL-18045

ON THE ORIGINS OF STRUCTURAL DEFECTS IN BF_2^+-IMPLANTED AND RAPID-THERMALLY-ANNEALED SILICON: CONDITIONS FOR DEFECT-FREE REGROWTH

T. Sands,[1] J. Washburn,[1] E. Myers[2]
and D. K. Sadana[2,3]

[1] Materials and Molecular Research Division
Lawrence Berkeley Laboratory
University of California
Berkeley, CA 94720

[2] North Carolina State University
Materials Engineering Department
Raleigh, NC 27650

[3] Microelectronics Center of North Carolina
P.O. Box 12889
Research Triangle Park, NC 27709

This work was supported by the Director, Office of Energy Research, Office of Basic Energy Sciences, Materials Science Division of the U.S. Department of Energy, under Contract No. DE-AC03-76SF00098.

ON THE ORIGINS OF STRUCTURAL DEFECTS IN BF_2^+-IMPLANTED AND RAPID-THERMALLY-ANNEALED SILICON: CONDITIONS FOR DEFECT-FREE REGROWTH

T. Sands,[1] J. Washburn,[1] E. Myers[2]
and D. K. Sadana[2,3]

[1]Materials and Molecular Research Division
Lawrence Berkeley Laboratory
University of California
Berkeley, CA 94720

[2]North Carolina State University
Materials Engineering Department
Raleigh, NC 27650

[3]Microelectronics Center of North Carolina
P.O. Box 12889
Research Triangle Park, NC 27709

ABSTRACT

The rapid thermal annealing behavior of BF_2^+-implanted silicon pre-amorphized with Si^+ and Ge^+ has been investigated with conventional and high-resolution cross-sectional transmission electron microscopy, and secondary-ion mass spectrometry. Three distinct layers of defects (types I, II and III) are identified. Fine clusters (type III) in the near-surface regions of both Si^+ and Ge^+ pre-amorphized samples are shown to be related to flourine. In addition, models for the nucleation of interstitial dislocation loops (type I) and "hairpin" dislocations (type II) are presented. These models and the experimental results suggest that the densities of type I and type II defects can be reduced by pre-amorphizing with Ge^+ instead of Si^+. Furthermore, defect-free regrowth is demonstrated for samples which are pre-amorphized with Ge^+ and rapid-thermally annealed at 1150°C.

1. Introduction

Ion implantation provides the control of dopant distributions necessary to reproducibly fabricate p-n junctions in silicon. However, the implantation of boron into single-crystal silicon for the purpose of creating shallow (< 0.5μm) p^+-n junctions presents several problems. For example, after high-dose (> $10^{15}cm^{-2}$) implantation of B^+ the wafer must be annealed at high temperatures ($\gtrsim$ 900°C) to activate the boron [1] and to eliminate implantation-induced defects. This implantation/diffusion treatment may result in significant boron in-diffusion and an undesirably deep junction [2]. Application of rapid annealing techniques can minimize dopant redistribution [3,4]. However, even if redistribution is negligible, the enhanced penetration of boron ions into single-crystal silicon due to crystallographic channeling places a lower limit on the junction depth [5] and thus may prevent the formation of the very shallow (~ 0.1μm) junctions desired for the scaled-down complementary metal-oxide-semiconductor (CMOS) technology.

In an effort to minimize the difficulties associated with obtaining B^+-implanted shallow junctions, an alternative shallow junction fabrication technique is currently being explored [5-15]. Rather than implantation of boron directly into single-crystal silicon, this alternative technique involves the "pre-amorphization" of the silicon surface layer (0.2-1.0μm) prior to dopant introduction. The following benefits may be realized by pre-amorphization: i) channeling of boron is eliminated since the target is amorphous [2,5]; ii) activation of

boron may be achieved at lower annealing temperatures since the boron is incorporated on substitutional sites during solid-phase epitaxial regrowth of the amorphous layer ($T > 550^{\circ}C$) [6]; and iii) if implantation-induced defects can be avoided or if they can be confined to a region well below the desired junction depth, then a boron drive-in step may not be necessary and rapid annealing techniques may be employed.

As a further perturbation to implantation of B^+ directly into single-crystal silicon, the boron may be introduced by implantation of BF_2^+. In this way, an equivalent boron distribution can be achieved by implantation at higher energies (11/49 of the beam energy is transferred to boron) and higher beam currents, thereby circumventing some practical problems asssociated with extracting a B^+ beam at low energy ($\lesssim 10$ keV) [16].

Recently, shallow junction formation by BF_2^+ implantation into Si^+-pre-amorphized substrates followed by rapid thermal annealing (RTA) with an incoherent light source has been investigated [8-10], Seidel et al. [11], and Sadana et al. [12-13] have demonstrated that pre-amorphization by Ge^+ implantation may have some advantages over pre-amorphization by self (Si^+) implantation. In particular, Ge^+ implantation results in lower defect densities and is an inherently simpler process since, unlike self implantation, only a single-step Ge^+ implantation is required to create an amorphous layer which extends to the surface [11-13].

In this paper, the origins of the various defects formed in Ge^+-pre-amorphized, BF_2^+-implanted and rapid-thermally-annealed silicon are investigated with a combination of secondary-ion mass spectrometry (SIMS) and cross-sectional transmission electron microscopy (XTEM). Emphasis is placed on processing conditions which prevent defect formation.

2. Experimental Methods

Surface layer amorphization of (100) silicon wafers to depths of 350-900nm was accomplished by either triple-energy Si^+ implantation (350, 150 and 70 keV to doses of 10^{16}, $2x10^{15}$ and $5x10^{15}cm^{-2}$, respectively) or single-step Ge^+ implantation (300 keV to doses of 10^{15} to $10^{16}cm^{-2}$). A continuous amorphous layer could be formed by Ge^+ implantation at (nominal) room temperature (RT). However, a continuous amorphous layer could be formed by self implantation only at (nominal) liquid nitrogen temperature (LNT) with a good thermal contact. Following pre-amorphization, the shallow boron distribution was obtained by implantation of 42 keV BF_2^+ to doses of $2x10^{15}$ to $10^{16}cm^{-2}$ at either RT or LNT. Solid-phase epitaxial regrowth of the amorphous layer was induced by RTA with incoherent light at temperatures of 950-1150°C for 10 seconds. The distributions of boron and flourine before and after RTA were obtained by SIMS (Cameca IMS, Model 3F). Plan-view TEM and XTEM allowed the determination of defect distributions. Specimens for XTEM were prepared by argon ion milling at LNT (5kV, specimen current ~ 20μA, 15° tilt). Cross-sectional high-resolution TEM (XHRTEM) was performed with a JEOL 200-CX (spherical

aberration coefficient, C_s = 1.2mm) at 200 keV. A through-focal series of high-resolution images was recorded for each area of interest in <110> zone-axis orientation with an objective aperture which contained nine beams. Images recorded at defocus values in the range of -70 to -90nm were selected for presentation below.

3. Results

As observed for samples pre-amorphized with Si^+ [9,10], three distinct layers of defects were found in Ge^+-amorphized, BF_2^+-implanted and rapid-thermally-annealed silicon. Employing the nomenclature of references [9] and [10], these defect layers are denoted as follows: type I, interstitial loops near the original amorphous-crystalline interface; type II, "hairpin" dislocations with a characteristic "V" shape; and type III, near-surface defects in the form of small clusters (1.5-4nm in diameter) and stacking faults bounded by Shockley partial dislocations.

Figure 1a is an XTEM image of a sample which was pre-amorphized with Ge^+, implanted with BF_2^+ to a dose of $2x10^{15}cm^{-2}$ at RT and then rapid-thermally-annealed at 1100°C. Interstitial Frank loops (type I) are clearly visible at a depth of ~ 400nm (approximately the depth of the amorphous-crystalline interface before annealing). This layer of loops was found to be present in samples annealed at temperatures of 1100°C and below. However, TEM images of Ge^+-implanted samples subjected to RTA at 1150°C (Fig. 2) revealed a complete absence of type I defects. This is in contrast to Si^+-implanted samples which contain a high density of type I defects after RTA at 1150°C [9,10].

Another significant difference between Ge^+-implanted and Si^+-implanted samples is that the density of type II defects (not shown) was observed to be substantially lower for the Ge^+-implanted samples [11-13]. For example, RTA at 950-1150°C of Si^+ and BF_2^+ (at RT)-implanted samples resulted in hairpin dislocation densities of ~ $2x10^8 cm^{-2}$ whereas the hairpin density in Ge^+-implanted samples subjected to the same BF_2^+ implant and RTA treatment was found to be < $10^7 cm^{-2}$.

Along with these dramatic differences in annealing behavior, the structural characteristics of the amorphous-crystalline interfaces in Ge^+ and Si^+-implanted samples before RTA were observed to be very different. Figure 3 compares the amorphous-crystalline interfaces in samples implanted with Si^+ and Ge^+ at LNT. It is clear that the amorphous-crystalline interface in Ge^+-implanted silicon is much more abrupt than in the self-implanted case. This difference is even more extreme for higher implantation temperatures (images not shown); silicon implanted at RT with Ge^+ (300 keV, 10^{16}cm) contains an undulating but fairly abrupt interface (peak-to-valley depth difference ~ 7-10nm) whereas silicon self-implanted at LNT with a poor thermal contact can contain an amorphous-crystalline transition region on the order of 0.1μm wide.

Defects of types I and II could be observed even when the BF_2^+-implantation step was omitted. However, the third class of defects (near-surface defects) were found to be present only in BF_2^+ or F^+-implanted samples. Figure 4 shows the SIMS data from the sample

imaged in Fig. 1. The flourine profile after RTA at 1100°C shows a sharp peak at a depth corresponding to the band of clusters at $\overline{R}_p \pm \Delta R_p$ in figure 1 ($\overline{R}_p$ is the mean projected range, ΔR_p is the corresponding standard deviation). Figure 1c is a XHRTEM image from a depth of ~ 14nm. These clusters were also observed in samples which received the equivalent flourine implant, indicating that the clusters are indeed related to flourine.

The SIMS data for boron (Fig. 4) shows singificant in-diffusion of boron at 1100°C and segregation of boron to the thin surface oxide which forms during RTA in an oxidizing atmosphere [14]. This enhanced in-diffusion of boron in Ge^+-implanted samples inhibits the formation of the near-surface stacking faults which are present in high densities ($1x10^9$ - $5x10^{10}cm^{-2}$) in self-amorphized samples [14]. These near-surface defects (type III) are described in more detail in reference [14] and will not be discussed further here.

4. Discussion

A detailed mechanism for hairpin dislocation nucleation is presented in reference [15]. This model involves the formation of perfect dislocation half loops to accommodate slight misorientation of small crystallites located near the upper portion of the amorphous-crystalline transition region. The misoriented crystallites, acting as seeds for epitaxial growth during RTA, result in the diverging arms of the hairpin dislocations. This nucleation mechanism is consistent with the TEM observations in that broader amorphous-crystalline transition regions (containing a higher density of isolated and

slightly misoriented crystalline seeds) are expected to generate higher densities of hairpin dislocations during RTA. Thus, one can limit the hairpin density by maintaining an abrupt amorphous-crystalline interface throughout the processing steps prior to RTA [15]. In particular, amorphization with heavy ions (eq. Ge^+) and at low temperatures discourages the subsequent nucleation of hairpin dislocations.

As demonstrated in Fig. 2, the nucleation of type I defects can be avoided as well if Ge^+ is used for pre-amorphization and if the sample temperature reaches ~ 1150°C rapidly (~ 1 to 3 seconds) during RTA. Similar results have been observed for As^+-implants into silicon [4,17]. In the following section, a simple qualitative model for the dependence of type I defect nucleation on the interface abruptness and RTA temperature is presented.

Model for the coalescence of interstitials created during implantation. It is intuitively reasonable that the transfer of forward momentum via recoil of host silicon atoms during implantion will result in the creation of a net excess of self-interstitials in a region below $\bar{R}_p$. If these excess silicon atoms reside in amorphous material before or during subsequent annealing, they will add extra atomic layers during epitaxial regrowth. If the excess interstitials are generated in crystalline material, they will either diffuse to nearby sinks (eg. an amorphous-crystalline interface) or they will cluster to form the nuclei of interstitial loops. Consequently, the density of interstitial dislocation loops (either Frank-type,

$\vec{b} = \frac{a}{3}$ <111>, or perfect, $\vec{b} = \frac{a}{2}$ <110>) will be determined by the competition between diffusion to interstitial sinks and the nucleation rate of interstitial loops.

Basic nucleation theory [18] shows that there exists a maximum nucleation rate at some temperature, T_{max}, below the melting temperature. At temperatures below T_{max}, the nucleation rate is limited by diffusion. As the temperature is increased above T_{max}, the nucleation rate drops since the critical cluster size required to form a nucleus (in unstable equilibrium) increases. Implicit in this model is the assumption that the equilibrium concentration of interstitials increases with temperature in the temperature range of interest. Given the above, one would expect that interstitial loop nucleation might be inhibited during annealing if the time spent in the temperature range near T_{max} were minimized, especially if efficient interstitial sinks were present nearby. Experimentally, this situation would correspond to the case of Ge^+-pre-amorphized samples rapid-thermally-annealed at 1150°C (Fig. 2; type I defects absent). One must also consider the possibility that interstitial loops may have been nucleated but were annealed out during the 10 seconds at 1150°C. However, the absence of dislocation residue from defect interactions and the fact that loops are still observed after RTA at 1150°C of Si^+-implanted samples, suggests that the loops were never nucleated in the Ge^+-implanted samples annealed at 1150°C. The presence of interstitial loops in the samples annealed at or below 1100°C indicates

that the nucleation rate is sufficiently high (and/or that the gettering efficiency of the amorphous-crystalline interface is sufficiently low) such that interstitial loop nucleation cannot be avoided.

The above discussion pertains to the case of a relatively abrupt amorphous-crystalline interface. However, the amorphous-crystalline interface can be very rough in Si^+-implanted samples (Fig. 3a). In these Si^+-implanted samples, the efficiency of the amorphous-crystalline interface as an interstitial sink is increased because of the greatly increased interface area. For example, it would be very unusual for an interstitial loop to nucleate within a small crystalline island. Therefore, while the crystalline material grows from all directions in the initial stages of annealing, the excess silicon atoms are rejected to the amorphous material. As the amorphous zones between growing islands shrink and disappear, the excess silicon atoms coalesce to form interstitial dislocation loops. The result is a spatial distribution of interstitial loops which reflects the width of the original amorphous-crystalline transition region. Further annealing will, of course, lead to coarsening of the interstitial loop distribution.

5. Summary

Pre-amorphization with Ge^+ has the following advantages over pre-amorphization with Si^+:

(1) Pre-amorphization with Ge^+ is a single-step process which can be accomplished at RT.

(2) The abruptness of the amorphous-crystalline interface in Ge^+-implanted samples results in a lower density of hairpin dislocations ($< 10^7 cm^{-2}$).

(3) This abrupt interface also helps to inhibit interstitial loop nucleation during RTA at 1150°C. Similar annealing conditions for Si^+-pre-amorphized samples result in the trapping of excess silicon in the rough transition region during annealing, thereby forcing interstitial loop formation as the amorphous zones within the transition region shrink.

To conclude, the results of this study suggest that Ge^+-pre-amorphization and B^+ implantation followed by RTA at 1150°C is a promising technique for producing defect-free boron-implanted shallow junctions.

The authors would like to thank Dr. J. Wortman for providing the pre-amorphized substrates and Drs. W. Maszara and G. Rozgonyi of the Materials Engineering Department, North Carolina State University, for useful discussions. The assistance provided by the staff of the National Center for Electron Microscopy, Lawrence Berkeley Laboratory, is also greatly appreciated. This work was supported by the Director, Office of Energy Research, Office of Basic Energy Sciences, Materials Science Division of the U.S. Department of Energy, under Contract No. DE-AC03-76SF00098.

References

[1] W. K. Hofker, Implantation of Boron in Silicon, Philips Res. Reports Suppl., No. 8 (Philips, Eindhoven, 1975) p. 15.

[2] R. G. Wilson, J. Appl. Phys. 54 (1983) 6879.

[3] J. L. Benton, G. K. Celler, D. C. Jacobson, L. C. Kimerling, D. J. Lischner, G. L. Miller and Mc. D. Robinson, in: 1981 Laser and Electron Beam Interactions with Solids, eds., B. R. Appleton and G. K. Celler (Elsevier, North-Holland, New York, 1982), p. 765.

[4] D. K. Sadana, S. Shatas and A. Gat, Proc. Inst. Phys. Conf. Ser. No. 67, Section 3 (1983) 143.

[5] T.-Y. Liu, Ph. D. Thesis, University of Caifornia, Berkeley (1983) Ch. 5.

[6] B. L. Crowder, J. F. Ziegler and G. W. Cole, in: Ion Implantation in Semiconductors and Other Materials, ed., B. L. Crowder (Plenum, New York, 1973) p. 257.

[7] M. Y. Tsai and B. G. Streetman, J. Appl. Phys. 50 (1979) 183.

[8] T. E. Seidel, IEEE Electron Dev. Lett., EDL-4, 10 (1983) 353.

[9] W. Maszara, C. Carter, D. K. Sadana, J. Liu, V. Ozguz, J. Wortman and G. A. Rozgonyi, Proc. of Mat. Res. Soc.; Energy Beam-Solid Interactions and Transient Thermal Processing (1983) in press.

[10] C. Carter, W. Maszara, D. K. Sadana, G. A. Rozgonyi, J. Liu and J. Wortman, Appl. Phys. Lett. 44 (1984) 459.

[11] T. Seidel, R. Knoell, F. A. Stevie, G. Poli and B. Schwartz, Proc. Spring Meeting of Electrochemical Society, Vol. 84-1 (1984) in press.

[12] D. K. Sadana, W. Maszara, J. J. Wortman, G. A. Rozgonyi and W. K. Chu, Journal of Electrochem. Soc., 131 (1984) 943.

[13] D. K. Sadana, E. Myers, J. Liu, T. Finstead and G. A. Rozgonyi, Proc. of Mat. Res. Soc.; Energy Beam-Solid Interactions and Transient Thermal Processing (1983) in press.

[14] T. Sands, J. Washburn, R. Gronsky, W. Maszara, D. K. Sadana and G. A. Rozgonyi, Appl. Phys. Lett. (1984), in press.

[15] T. Sands, J. Washburn, R. Gronsky, W. Maszara, D. K. Sadana and G. A. Rozgonyi, Journal of Electronic Materials (Proc. 13th Int. Conf. on Defects in Semiconductors, 1984) in press.

[16] H. Müller, H. Ryssel and I. Ruge, in: Ion Implantation in Semiconductors, eds., I. Ruge and J. Graul (Springer-Verlag, Berlin, 1971), p. 85.

[17] J. Narayan and R. T. Young, Appl. Phys. Lett., 42 (1983) 466.

[18] D. A. Porter and K. E. Easterling, Phase Transformations in Metals and Alloys (Van Nostrand Reinhold, Wokingham, 1981) Chapters 4 and 5.

FIGURE CAPTIONS

Fig. 1. Cross-sectional TEM images of Ge^+-pre-amorphized, BF_2^+-implanted (42 keV, $2x10^{15}cm^{-2}$) and rapid-thermally-annealed (1100°C, 10 sec) silicon;

a) Bright-field ($\vec{g}$ = 220) image showing near-surface band of clusters and deep layer of interstitial loops.

b) Stacking faults near oxide-silicon interface imaged by XHRTEM.

c) XHRTEM image of fine clusters at depth of ~ 14nm.

Fig. 2. Cross-sectional TEM images of Ge^+-pre-amorphized, rapid-thermally annealed (1100 and 1150°C, 10 sec) silicon. Note absence of type I defects in sample annealed at 1150°C.

Fig. 3. High-resolution XTEM images of amorphous-crystalline interface in;

a) Si^+-pre-amorphized and

b) Ge^+-pre-amorphized silicon. Both implants performed at LNT with good thermal contact.

Fig. 4. Boron and flourine depth distributions (SIMS) of sample imaged in Fig. 1.

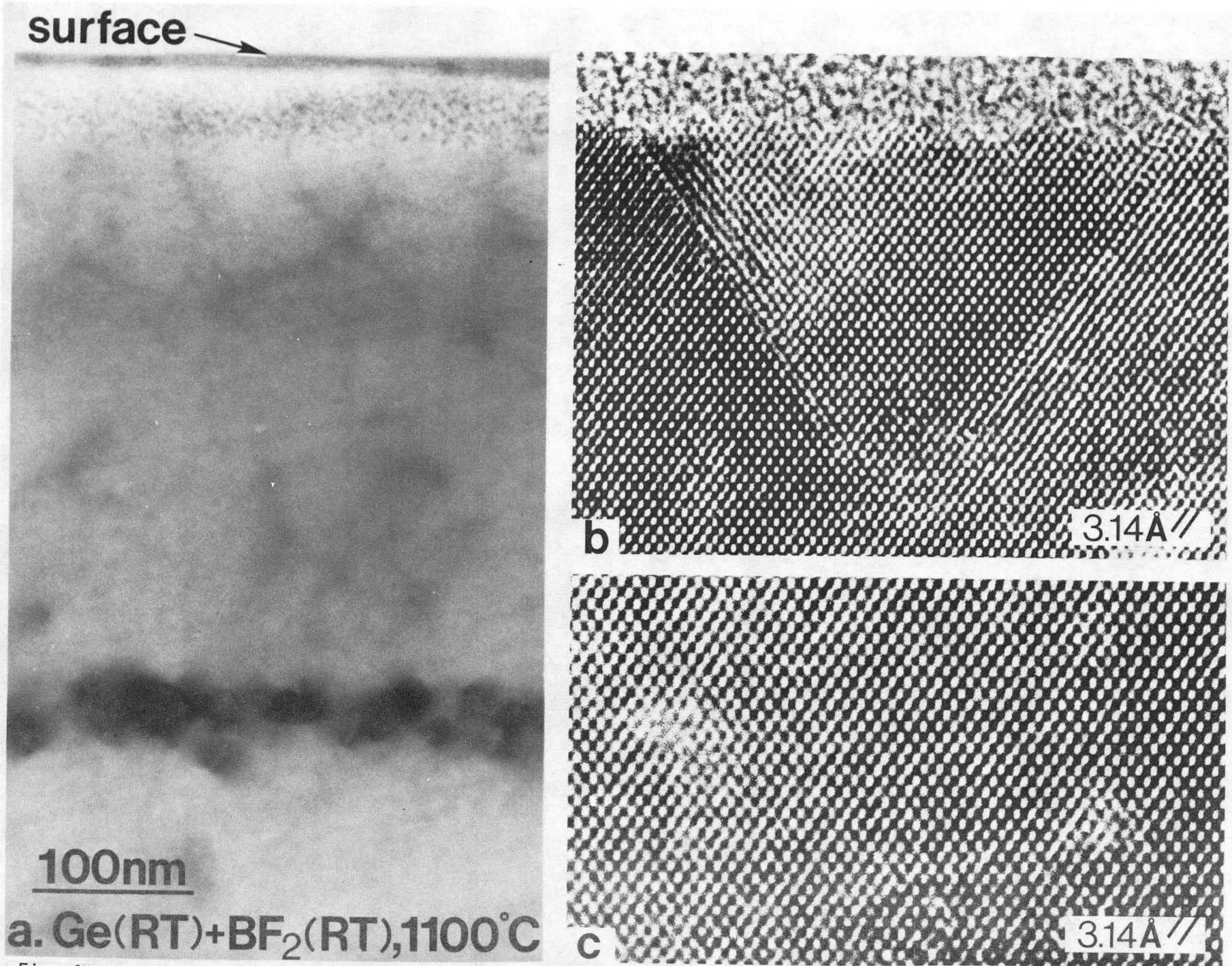

Fig. 1

XBB 845-3281

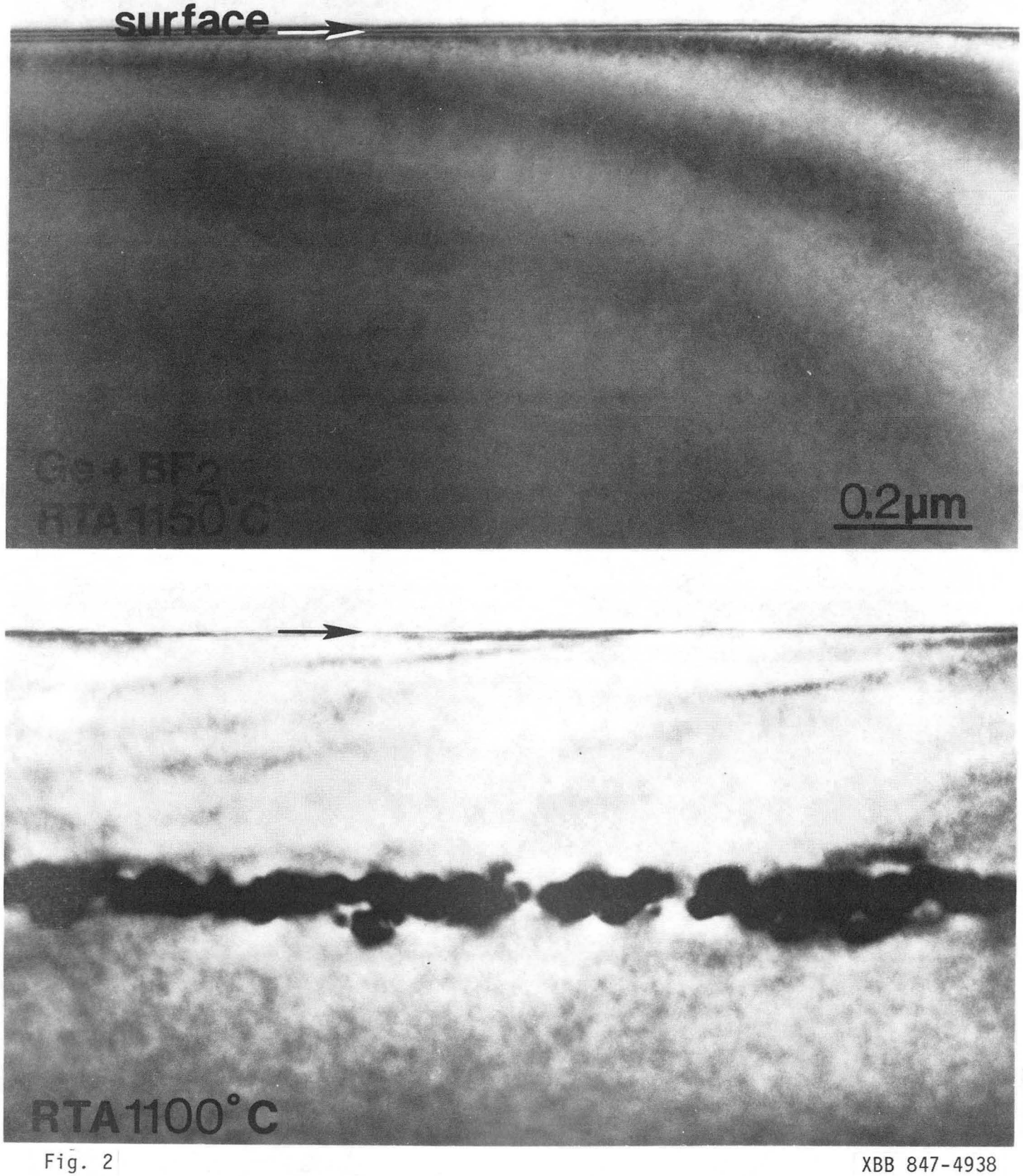

Fig. 2

XBB 847-4938

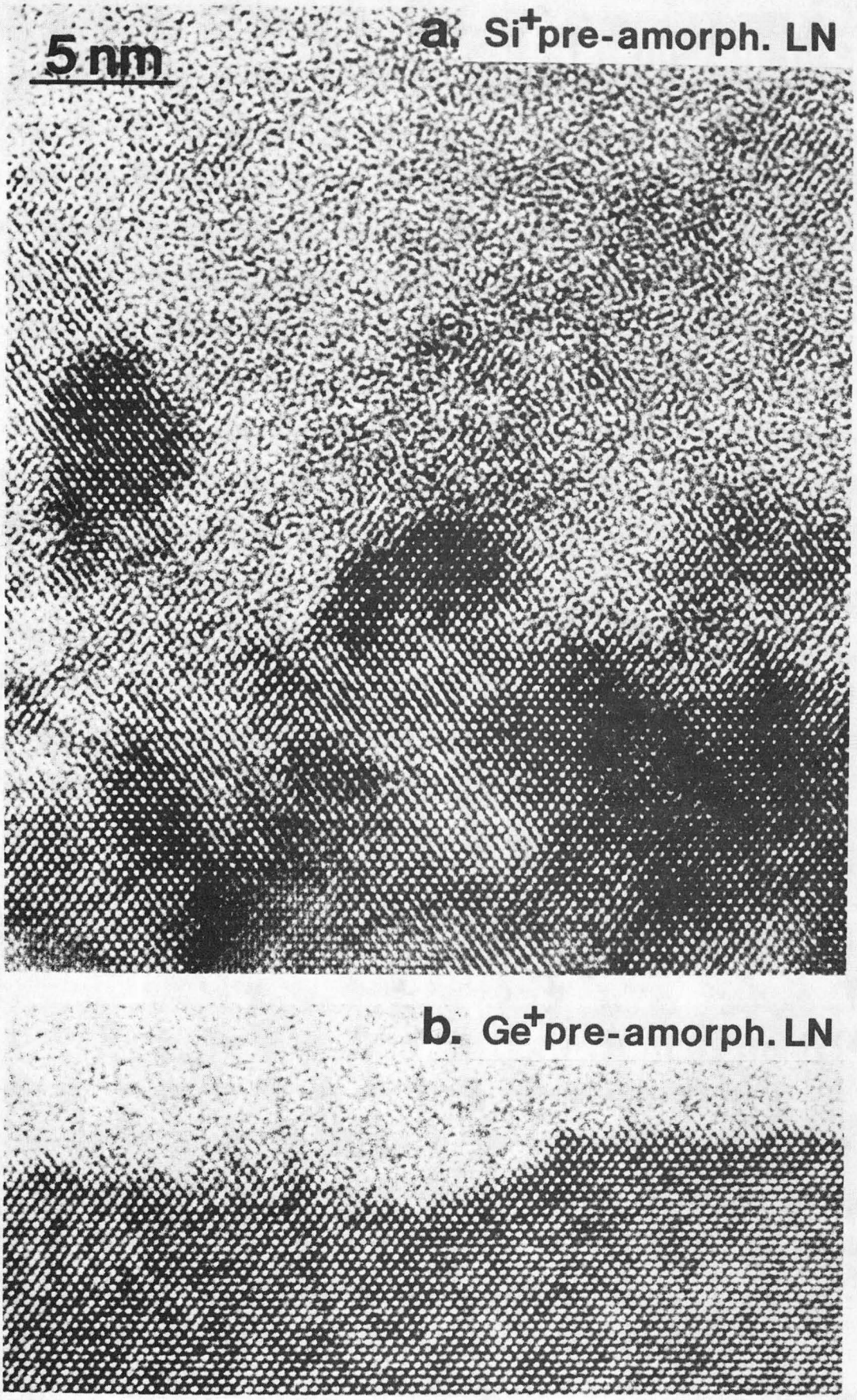

Fig. 3

XBB 846-4778

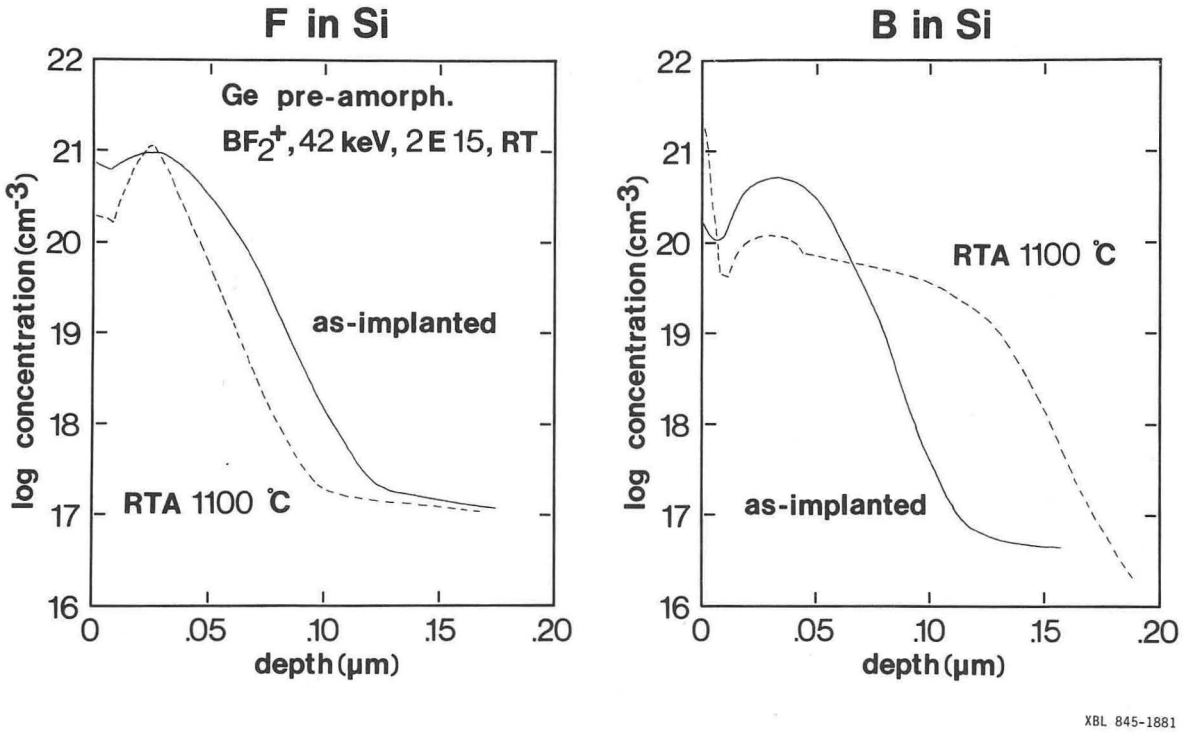
F in Si
Ge pre-amorph.
BF2+, 42 keV, 2 E 15, RT
as-implanted
RTA 1100 °C
log concentration (cm-3)
depth (μm)
B in Si
RTA 1100 °C
as-implanted
log concentration (cm-3)
depth (μm)
XBL 845-1881

Fig. 4

This report was done with support from the Department of Energy. Any conclusions or opinions expressed in this report represent solely those of the author(s) and not necessarily those of The Regents of the University of California, the Lawrence Berkeley Laboratory or the Department of Energy.

Reference to a company or product name does not imply approval or recommendation of the product by the University of California or the U.S. Department of Energy to the exclusion of others that may be suitable.

TECHNICAL INFORMATION DEPARTMENT
LAWRENCE BERKELEY LABORATORY
UNIVERSITY OF CALIFORNIA
BERKELEY, CALIFORNIA 94720